Available online at www.sciencedirect.com
ScienceDirect
Trans. Nonferrous Met. Soc. China 33(2023) 1932−1942
Transactions of Nonferrous Metals Society of China
www.tnmsc.cn

Kinetics of alumina extraction from coal gangue by hydrochloric acid leaching

Yu-juan ZHANG[1,2], Jun-min SUN[1,2], Guo-zhi LÜ[3], Ting-an ZHANG[3], Yan-bing GONG[1,2]

1. College of Chemical Engineering, Inner Mongolia University of Technology, Hohhot 010051, China;
2. National and Local Joint Engineering Research Center for High Value Utilization of Coal-based Solid Waste, Hohhot 010051, China;
3. Key Laboratory of Ecological Metallurgy of Multi-metal Intergrown Ores of Ministry of Education, Special Metallurgy and Process Engineering Institute, Northeastern University, Shenyang 110819, China

Received 26 January 2022; accepted 11 April 2022

Abstract: The leaching kinetics of alumina extraction from coal gangue with hydrochloric acid was investigated. The effects of calcination activation temperature and leaching conditions on the alumina extraction efficiency were studied. The results revealed that the alumina extraction efficiency can reach 91.56% under the following optimum conditions: a calcination temperature of 700 °C, dissolution at 150 °C for 2 h in hydrochloric acid with a concentration of 20%, and a liquid-to-solid ratio of 3:1. Notably, lithium was leached simultaneously with alumina, and its leaching rate reached 80.00 %. The leaching of alumina followed the shrinking unreacted core model, and the process was controlled by a chemical reaction, with activation energy of 45.64 kJ/mol.

Key words: coal gangue; acid leaching; calcination activation; leaching kinetics; alumina

1 Introduction

Coal is the most abundant and widely distributed fossil fuel on earth. And coal gangue is a type of solid waste discharged during the coal mining and washing process; its main components are SiO_2 (52%−65%) and Al_2O_3 (16%−36%). Over 5 billion tons of coal gangues have been accumulated in China, and this amount is still increasing at an annual rate of 300−350 million tons [1,2]. Such vast amounts of coal gangues have various impacts on soil, air, and groundwater [3,4]. Since the 1960s, coal gangue has been used in many countries for paving, power generation, brick making [5−7], and building materials [8−10]. The total amount of high-aluminum coal gangue produced during the mining of high-aluminum coal in the Zhungeer mining area, Inner Mongolia, exceeds 6 million tons, and its alumina content exceeds 40%. Thus, coal gangue can be used as an alternative resource for the production of aluminum-based chemical products for high-value utilization [11−13].

Currently, methods for extracting aluminum from coal gangue include acid leaching [14], alkaline leaching [15], and hydrochemical methods [16,17]. The acid leaching method has been extensively studied owing to its high alumina extraction rate, small number of tailings, and short process time. Coal gangue must be activated in advance to improve the material activity, and this process can be divided into mechanical and calcination activations [18,19]. Calcination at 650−1050 °C results in the removal of bound water from kaolinite ($Al_2O_3·SiO_2·2H_2O$) and conversion to metakaolinite ($Al_2O_3·2SiO_2·2H_2O$), which has

Corresponding author: Yan-bing GONG, Tel: +86-18104711669, E-mail: gongyb@imut.edu.cn
DOI: 10.1016/S1003-6326(23)66233-8

poor crystallinity and high activity [20,21], and the loss of activity because of the recrystallization into mullite at heating temperatures above 1000 °C [22,23]. Consistent with this, the dissolution contents of SiO_2 and Al_2O_3 are 92.31% and 64.44%, respectively, at a calcination temperature of 700 °C [24]. The dissolution rate of alumina can be greatly improved by adding limestone during calcination; furthermore, sodium carbonate can react with coal gangue to form nepheline during calcination, increasing the solubility of alumina in acid [25]. Comparing the influence of different calcination atmospheres on the dissolution rate of alumina, air was found to have a better activation effect [26].

A kinetic study of coal gangue leaching by sulfuric acid has shown that the reaction is controlled by an interfacial chemical reaction [27], and the process of leaching aluminum from coal-series kaolinite is controlled by a chemical reaction [28]. The combustion properties and kinetic behavior of coal gangue were systematically investigated under an air atmosphere [29]. In studies on low-grade aluminum resources, much attention has been paid to the dissolution of aluminum and iron materials, such as fly ash [30,31], low-grade kaolinite [32], aluminum dross [33], red mud [34], and high-silica bauxite [35,36]. Although there have been many reports on the extraction of alumina from coal gangue [37,38], there are few studies on the kinetics of the hydrochloric acid leaching process, especially segmented and refined studies on the dissolution kinetics of hydrochloric acid.

In response to the above problems, the kinetics of the aluminum leaching process was explored in detail, providing a reference for the optimization of the extraction of alumina from coal gangue by hydrochloric acid leaching. A new kinetics model was preliminarily established, and the mechanism of the dissolution process of hydrochloric acid was investigated in depth.

2 Experimental

2.1 Materials

The coal gangue used in this study was obtained from Buliangou, Zhungeer Banner, Ordos City, Inner Mongolia Autonomous Region, China.

2.2 Methods

The coal gangue was crushed into small pieces of 1−2 cm using a hammer, inserted into the crusher, crushed for 1 min, passed through 60 mesh standard sieve, dried for 2 h at 105 °C, and stored in a bag for use (see Fig. 1).

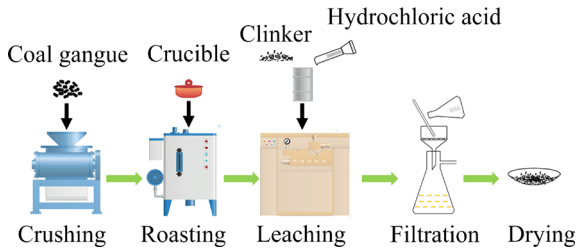

Fig. 1 Schematic of calcination activation−hydrochloric acid leaching process

Coal gangue (50 g) was spread on a crucible that was inserted into a muffle furnace. The temperature was increased by 10 °C/min and maintained at 300−900 °C for 2 h; the sample was then cooled to room temperature and removed for later use. In this step, bound water and volatile components (mostly carbon) were removed from coal gangue.

30 g of clinker was mixed with hydrochloric acid (5%, 10%, 15%, 20%, 25%, and 30%) and deionized water according to liquid-to-solid ratios of 1:1, 2:1, 3:1, 4:1, and 5:1 (30, 60, 90, 120, and 150 mL) in the pressure-dissolved bomb of homogeneous reactor. The speed of stirring was set to 10.5 r/min, the temperature was increased by 5 °C/min and maintained at 75, 95, and 150 °C for 2 h.

After the reaction was complete, the hot filtrate was washed 4−5 times with hot water. The leached residue was then dried and subjected to inductively coupled plasma (ICP) analysis.

The alumina extraction efficiency (η, %) was calculated using Eq. (1):

$$\eta = \frac{m_1 A_1 - m_2 A_2}{m_1 A_1} \tag{1}$$

where m_1 is the mass of the clinker (g), A_1 is the alumina content in the clinker (%), m_2 is the mass of the leaching residue (g), and A_2 is the alumina content of the leaching residue (%).

2.3 Characterization techniques

X-ray diffraction analysis (XRD, D/MAX 2500PC, Rigaku Corporation) was used to analyze

the mineral composition of the samples using a Cu K_α source, DS=SS=1°, RS=0.3 mm, 2θ scan: 5−90°, and scanning speed = 30 (°)/min. X-ray fluorescence spectrometry (Rigaku Corporation) was used to analyze the chemical compositions of the samples. The morphology and microstructure of the samples were observed using a SIRION200 scanning electron microscope (SEM). The STA 409PC thermal analytical balance (Germany) used N_2 as the baseline from ambient temperature to 1200 °C at a rate of 15 °C/min. A Nicolet 6700 Fourier transform infrared spectrometer (USA) was used for the Fourier transform infrared spectroscopy (FTIR). The samples were mixed with KBr and measured in the range of 400−4000 cm^{-1}. The Li content was determined using an Avio 200 ICP spectrometer (PE Company).

3 Results and discussion

3.1 Composition of raw material

The chemical composition of the raw material is shown in Table 1, in which the presence of the trace element Li is observed in addition to the major elements of aluminum and silicon.

Table 1 Chemical composition of coal gangue (wt.%)

SiO_2	Al_2O_3	Fe_2O_3	CaO	MgO	TiO_2	K_2O	Li	LOI
45.8	38.21	0.73	0.5	0.51	0.84	0.20	0.02	13.1

The mineral compositions analyzed by XRD showed that the main phase of the coal gangue was kaolinite (Fig. 2(a)). Although the coal gangue generally contains a quartz peak, it was not observed in the analyzed sample, which may be attributed to the low quartz content. The high intensity and sharpness of the diffraction peaks indicate good crystallinity. This stable phase structure hinders decomposition under the mild conditions; therefore, activation by calcination is required. TG-DTA test results (Fig. 2(b)) showed that coal gangue has a sharp mass loss at approximately 700 °C, moreover, the endothermic peak caused by the removal of hydroxyl groups occurred at 515 °C, and the exothermic peak of spinel crystal phase transformation occurred at 1000 °C.

3.2 Effect of reaction conditions on alumina extraction efficiency

3.2.1 Effect of acid concentration and liquid-to-solid ratio

The alumina extraction efficiency increased with increasing HCl concentration, as shown in Fig. 3(a). With an increase in the HCl concentration, the contact between H^+ and coal gangue particles increased, providing a more efficient reaction and higher alumina extraction rate. The liquid-to-solid ratio had a considerable influence on the alumina extraction efficiency and concentration of aluminum chloride after dissolution. Although a high liquid-to-solid ratio results in a high alumina extraction rate, the aluminum chloride solution formed has a low concentration and is difficult to utilize further; thus, the optimal liquid-to-solid ratio was 3:1, as shown in Fig. 3(b).

3.2.2 Effect of calcination activation and leaching temperature

The extraction rate of alumina is proportional to the leaching temperature, as shown in Fig. 4(a). As the acid leaching temperature increased, the pressure in the system increased, which was conducive to the destruction of the gangue mineral

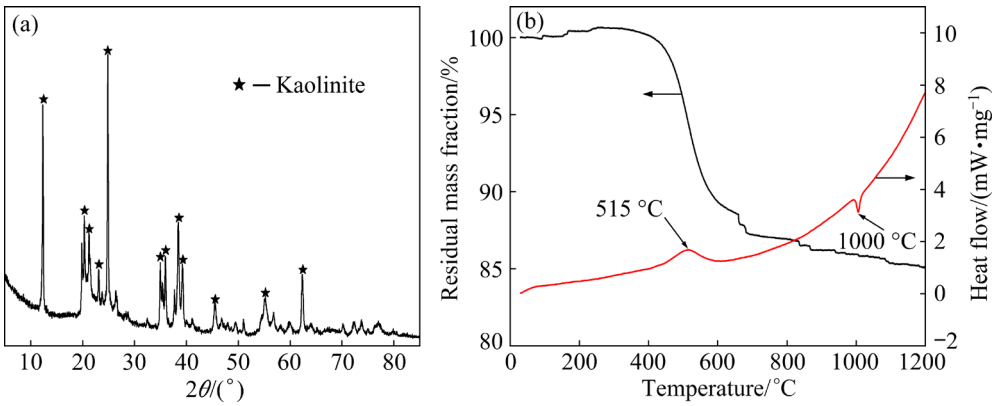

Fig. 2 XRD pattern (a) and TG-DTA analysis (b) of coal gangue

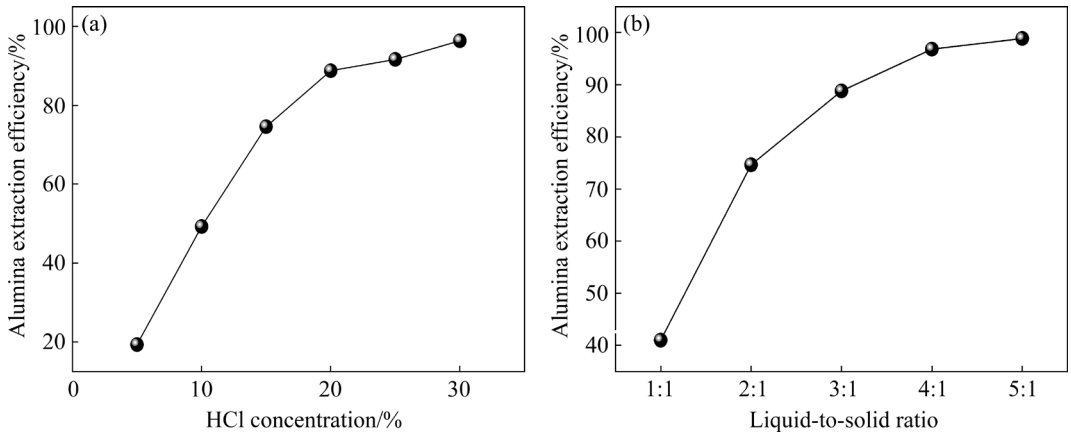

Fig. 3 Effect of acid concentration (a) (calcination at 700 °C, leaching at 150 °C for 2 h) and liquid-to-solid ratio (b) on alumina extraction efficiency (20% HCl)

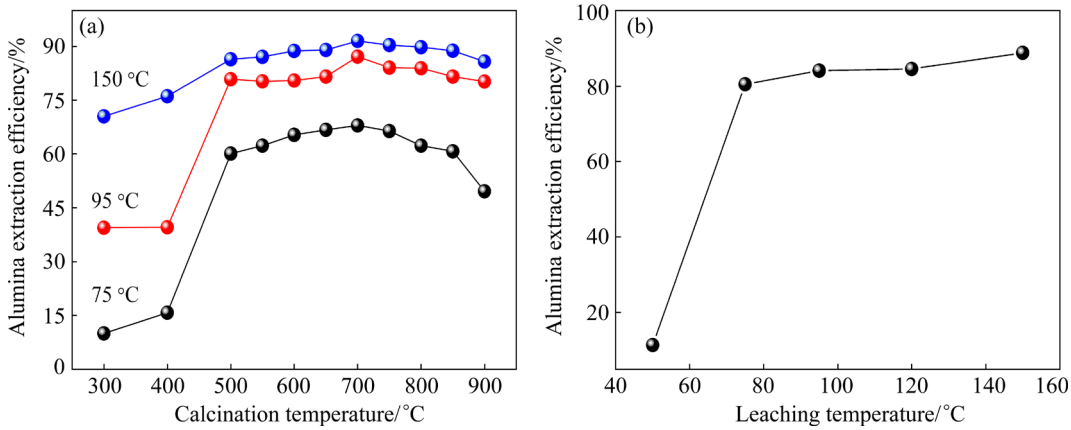

Fig. 4 Effect of calcination activation (a) and leaching temperature (calcination at 700 °C) (b) on alumina extraction efficiency (liquid-to-solid ratio = 3:1, leaching time = 2 h, 20% HCl)

structure: the number of reactive molecules increased, and the rate of molecular diffusion increased. Consequently, the dissolution rate of aluminum increases. The experimental results indicated that when the leaching temperature reached 150 °C, the alumina extraction efficiency was greater than 90% (Fig. 4(b)). However, with an increase in the calcination temperature, the leaching rate of aluminum first increased, then decreased, and reached a maximum at 700 °C. Coal gangue also contains a small amount of lithium, which is widely used in many fields. Lithium can be synergistically extracted during the extraction of aluminum such that coal gangue can achieve its maximum utilization value. Because of its low lithium content, lithium extraction from coal gangue is economically viable only when combined with aluminum extraction. Figure 5 clearly indicates that the leaching rate of lithium increases with an

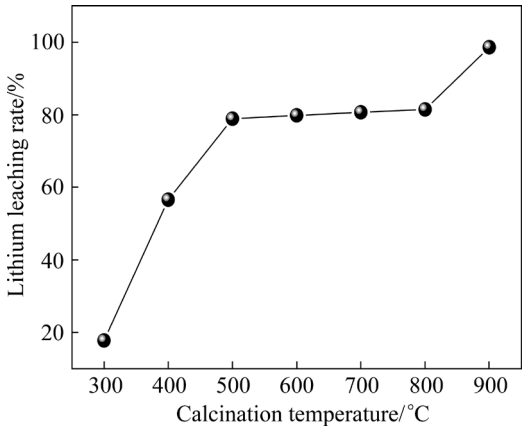

Fig. 5 Effect of calcination temperature on leaching rate of lithium

increase in the calcination temperature, and reaches more than 80% at a calcination temperature of 700 °C. However, it is interesting that when the calcination activation temperature reaches 900 °C,

the leaching rate of lithium reaches 98%, which indicates that the phase of coal gangue has changed at this time, and the reactivity of lithium is the highest at this time.

3.3 Kinetics of hydrochloric acid leaching

The reaction of coal gangue and hydrochloric acid solution is a typical liquid−solid non-catalytic reaction. The main phases in the raw materials were kaolinite and quartz. Only certain components of the raw materials were selectively leached as they reacted with hydrochloric acid, and a certain amount of solid residue was produced during the leaching process. According to the kinetic principle of hydrometallurgy, when some minerals in the raw materials cannot be leached and solid products are formed, the leaching process conforms to the "shrinking core model".

Based on the experiment before concentration selection, a linear velocity of 11 m/s can eliminate the diffusion effect. Therefore, we only need to consider the temperature and time to study the dynamic model. As shown in Fig. 6, the effect of temperature on the leaching rate of aluminum is considerable. In the 0−160 min period, the reaction rate decreases. The fitting data for the aluminum leaching reaction are shown in Fig. 7. After calcination, the leaching of alumina was controlled by a chemical reaction.

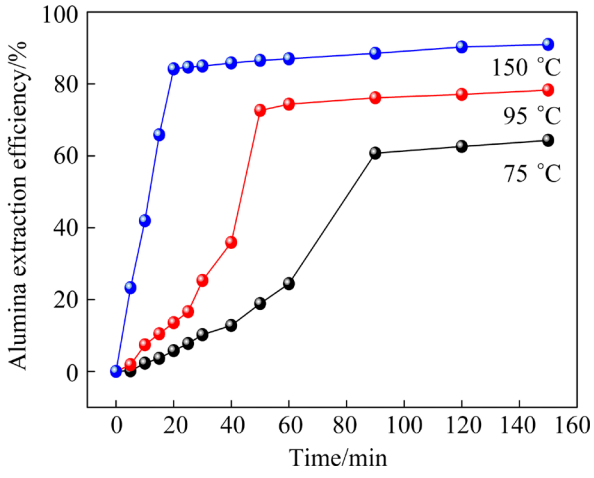

Fig. 6 Effect of reaction time and temperature on alumina extraction efficiency (leaching conditions: 20% HCl, liquid-to-solid ratio = 3:1)

The fitting results of the dynamic model show that the reaction was controlled by a chemical reaction in the temperature range of 75−150 °C. Under the experimental conditions, the kinetic equation can be written as

$$1-(1-\eta)^{1/3}=kt \quad (2)$$

where t is the reaction time, and k is the rate constant.

According to the Arrhenius equation, $k=A\exp[-E_a/(RT)]$, considering the logarithmic expression $\ln k = \ln A - E_a/(RT)$, and plotting the $\ln k$ versus $1/T$, as shown in Fig. 8, the result showed a good linear relationship. Based on the slope of the fitted curve, the activation energy is 45.64 kJ/mol.

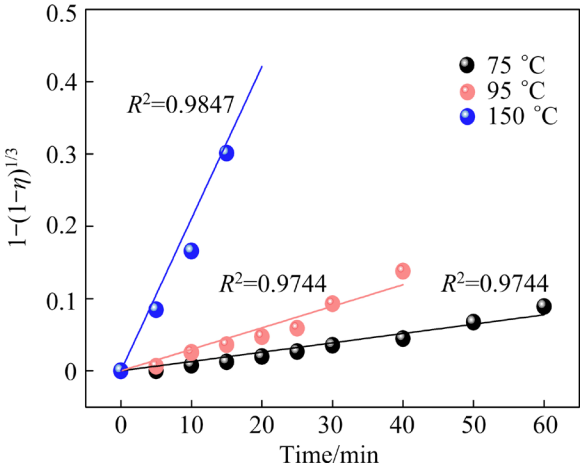

Fig. 7 Fitting of data of alumina leaching kinetics

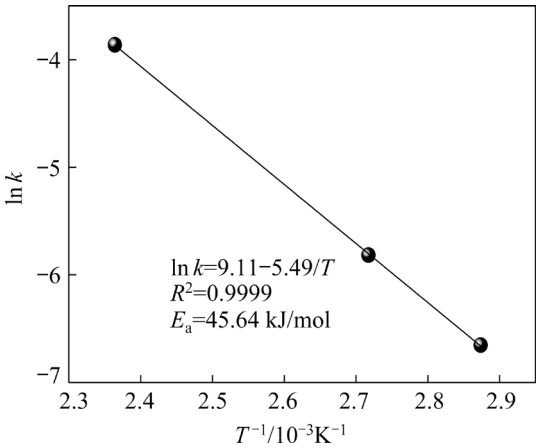

Fig. 8 Arrhenius plot of aluminum leaching kinetics

3.4 Reaction mechanism

Figure 9(a) shows the XRD patterns of coal gangue clinker at different calcination temperatures. Compared with the raw material, the calcined coal gangue phase considerably changed. The diffraction peak of kaolinite became very weak under the calcination temperature of 500 °C, which indicates that during the calcination, a large amount of kaolinite

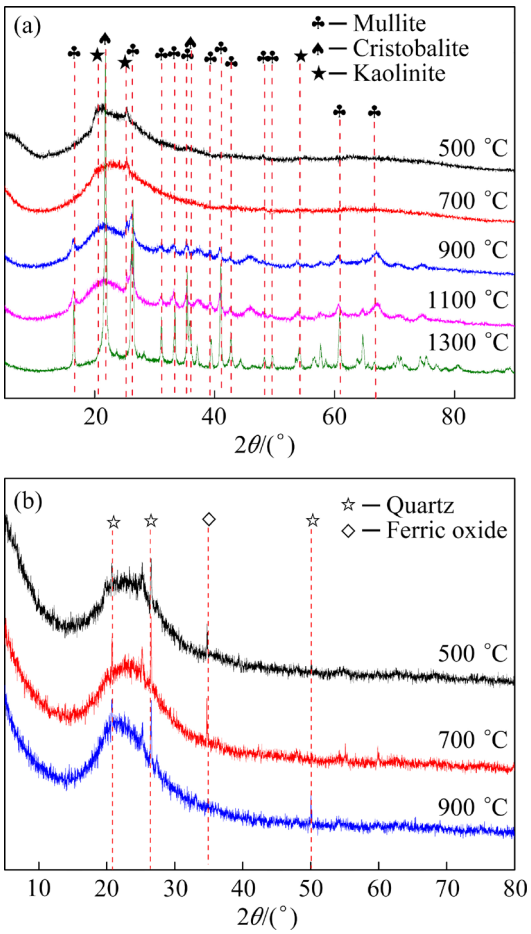

Fig. 9 XRD patterns of coal gangue clinker (a) and acid leaching slag (b)

was decomposed into metakaolinite [39,40]. With the increase of the calcination temperature to 700 °C, the diffraction peaks of kaolinite completely disappear, which indicates that the structure of kaolinite was completely destroyed, and kaolinite decomposition was completed. Interestingly, a broad peak appeared at 20°−25°, demonstrating that a non-crystalline substance was formed. However, with the increase of the calcination temperature to 900 °C, the mullite crystalline phase started to appear, with the corresponding peaks gradually intensifying with the further increase in temperature until 1300 °C, where it was completely crystallized, and the non-crystalline phase disappeared. Thus, the calcination resulted in kaolinite decomposition before 700 °C, and formation and growth of the mullite phase after 700 °C, and the coal gangue exhibited the highest activity after calcination at 700 °C.

The XRD patterns of the acid leaching residue under leaching conditions of 20% HCl, liquid-to-solid ratio 3:1, T=150 °C, and t=2 h are shown in Fig. 9(b). A broad peak appeared at 20°−25°, indicating that most of the alumina was leached, and only a large amount of silica remained.

Figure 10 shows the FT-IR analysis results of acid leaching slag and coal gangue clinker at different calcination temperatures. The absorption peaks at 3696 and 3622 cm^{-1} disappeared at the calcination temperature of 700 °C, as shown in Fig. 10(a). Thus, it can be concluded that the —OH in the kaolinite was completely removed, and kaolinite was converted into metakaolinite. The broadening of the absorption peaks at 1038 and 1096 cm^{-1} indicates that the tetrahedral structure of SiO_2 was destroyed; the broadening or disappearance of the absorption peaks at 920 and 543 cm^{-1} indicates that the Al—OH and Si—O—Al bonds were broken to form SiO_2 and γ-Al_2O_3, respectively. Figure 10(b) shows that as the calcination temperature increased, the —OH peaks at 3696 and 3622 cm^{-1}, Si—O—Al stretching vibration peaks at 694 cm^{-1}, and Al—OH bending

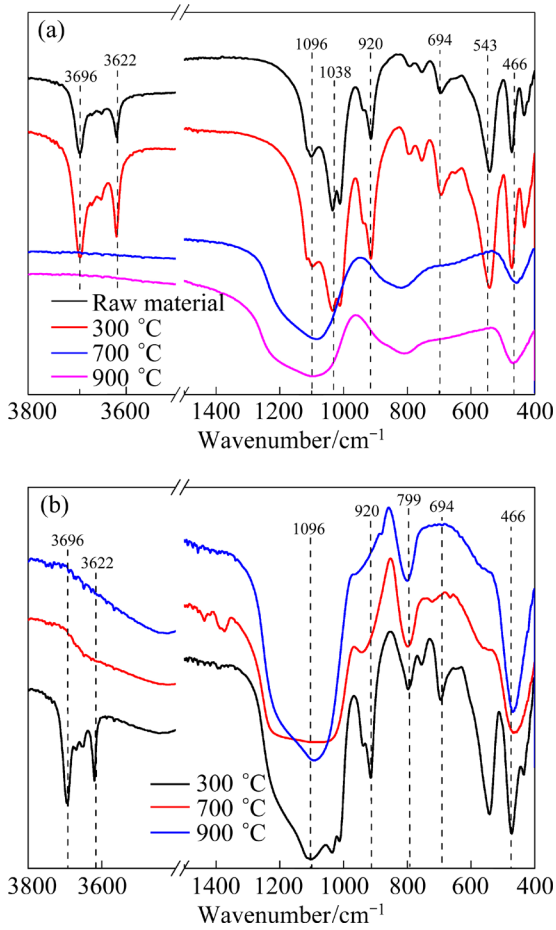

Fig. 10 FT-IR analysis of coal gangue clinker (a) and acid leaching slag (b)

vibration front at 920 cm^{-1} in the acid leaching residue disappeared; in contrast, Si—O related peaks at 1096, 799, and 466 cm^{-1} became stronger, which indicated that most of the alumina was leached, and the main component in the acid leaching residue was SiO_2.

After calcination, the coal gangue changed from a compact structure (Fig. 11(a)) to a loose structure (Fig. 11(b)), which was related to the transformation of kaolinite into metakaolinite. Figures 11(c−f) show the changes in particle morphology under different leaching time conditions. With an increase in leaching time, the gangue particles became more compact and their spherical particle size gradually decreased, which is consistent with the kinetic model "shrinking core model" adopted above. Figure 12 shows the results of the SEM−EDS analyses of the coal gangue raw materials and acid leaching slag. In the range of particle labeling, the energy spectrum analyses showed that the coal gangue contained 12.7 wt.% Al and 12.1 wt.% Si, whereas after the calcination activation-hydrochloric acid leaching, the slag contained 1.6 wt.% Al and 15.7 wt.% Si, indicating that most of Al leached and there was a reduction in mass.

It can be seen from Fig. 13 that the particle size distribution patterns of coal gangue before and after calcination are basically the same, but after leaching for 2 h with hydrochloric acid, not only did D_{50} become smaller, but the largest and smallest particles disappeared, and the particle size distribution was more concentrated.

The "shrinking core model" kinetic process of alumina leaching in coal gangue can be summarized as follows.

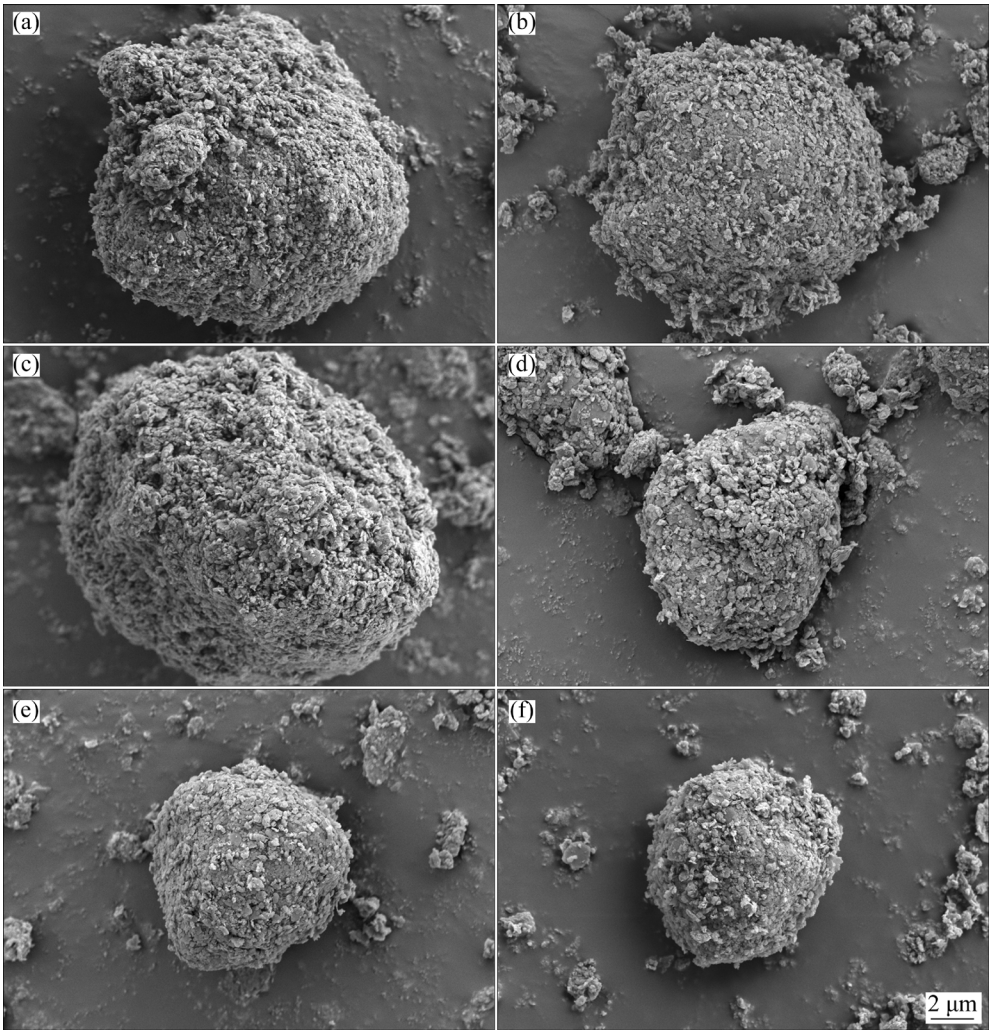

Fig. 11 SEM images of coal gangue during calcination−hydrochloric acid leaching: (a) Coal gangue; (b) Coal gangue clinker; (c) Leaching after 5 min; (d) Leaching after 20 min; (e) Leaching after 60 min; (f) Leaching after 120 min

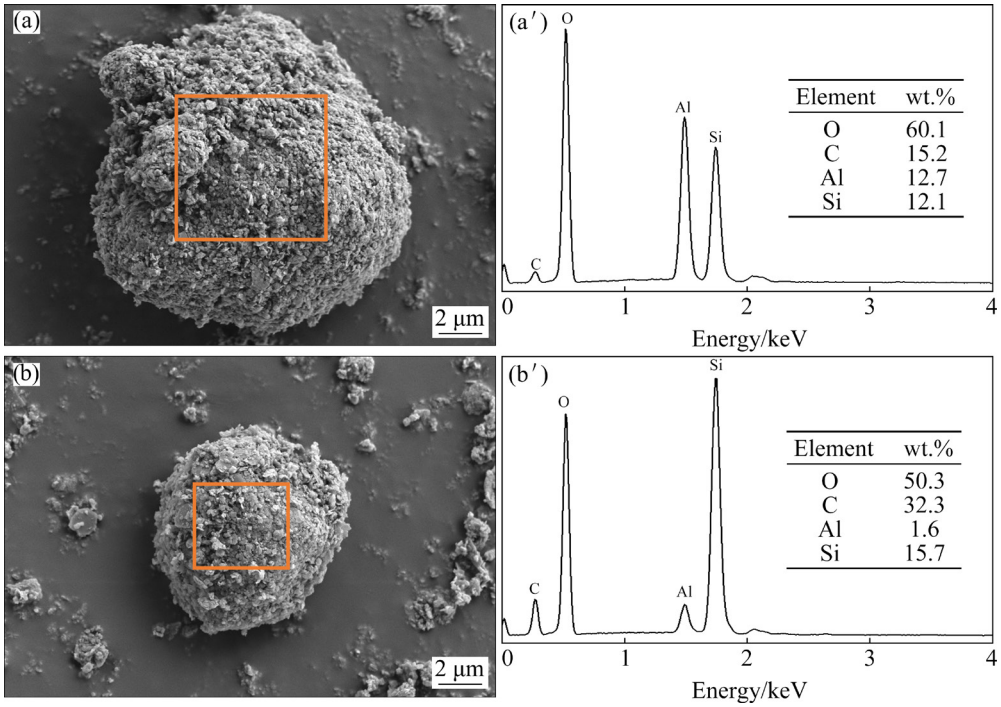

Fig. 12 SEM−EDS analysis of coal gangue (a, a′) and hydrochloric acid leaching slag (b, b′)

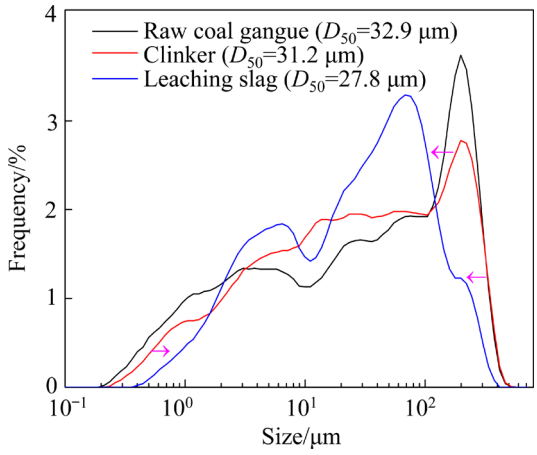

Fig. 13 Particle size distribution of coal gangue, clinker, and leaching slag

Step 1: Hydrochloric acid diffuses to the surface of coal gangue particles.

Step 2: Hydrochloric acid diffuses to the reaction interface of coal gangue particles.

Step 3: Hydrochloric acid reacts with aluminum minerals at the reaction interface.

Step 4: The reaction product aluminum chloride diffuses into the boundary layer.

Step 5: The reaction product aluminum chloride diffuses outward through the boundary layer.

Figure 14 shows the schematic of the kinetics of the calcination activation−hydrochloric acid leaching process of aluminum in coal gangue. Initially, after hydrochloric acid diffuses to the reaction interface through external diffusion, alkali metals such as aluminum, iron, and calcium in the coal gangue react with hydrochloric acid to form chloride and enter into the solution. With the dissolution of aluminum and contraction of Si not involved in the reaction, the overall particle diameter shrinks from r to r_1; this stage is mainly controlled by chemical reactions. As the reaction progresses, aluminum leaches into the solution, and after most of the aluminum is leached, the surface of the solid particles gradually becomes dominated by silicon as the particles shrink. At the same time, the diffusion of H^+ into the particles is hindered by the silicon product layer, and the reaction enters the second stage, which is mainly controlled by internal diffusion, and the particle radius r_1 remains unchanged until the reaction is complete.

3.5 Further treatment of solution

The leaching solution consisted mainly of aluminum chloride but also contained a small amount of impurities such as ferric chloride, calcium chloride, and magnesium chloride; most of the lithium also leached into the solution in the form of lithium chloride. The results of the chemical composition analyses are listed in Table 2.

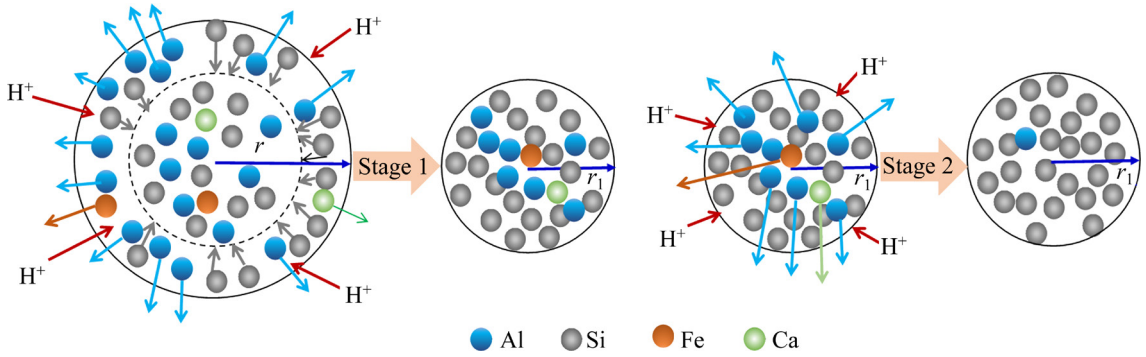

Fig. 14 Schematic of kinetics

Table 2 Chemical composition of leaching solution (g/L)

Al_2O_3	Fe_2O_3	CaO	MgO	TiO_2	Li
121.7	2.20	1.63	1.80	2.53	0.062

The most direct and economical method for the utilization of the solution is polymerization with calcium aluminate powder to generate poly aluminum chloride, which can be directly used in solution or dried as a water purifying agent product and directly used in the chemical industry, and water plants, etc. It can also be used to produce crystalline aluminum chloride for casting, production of pharmaceuticals and additives, and other purposes. High-purity alumina can be prepared through multiple crystallizations.

4 Conclusions

(1) The results revealed that the alumina extraction efficiency reached 91.56% under the optimum conditions (calcination at 700 °C for 2 h, hydrochloric acid concentration of 20%, liquid-to-solid ratio of 3:1, and leaching at 150 °C for 2 h). Simultaneously, the leaching rate of lithium reached 80.00%.

(2) Kinetic studies indicated that the hydrochloric acid leaching process is controlled by a chemical reaction with an activation energy of 45.64 kJ/mol.

(3) The mechanism analysis showed that kaolinite, the main aluminum-containing phase in the coal gangue, was converted into metakaolinite when the calcination temperature reached 700 °C, yielding the highest activity of the coal gangue and alumina extraction rate. However, with further increase in the calcination temperature, meta-kaolinite decomposed into mullite, resulting in a decrease in the extraction rate of alumina. The acid leaching reaction contained amorphous SiO_2, and most of the Al_2O_3 was leached.

Acknowledgments

This research was supported by the National Key R&D Program of China (No. 2021YFE0102200), the Inner Mongolia Natural Science Foundation, China (No. 2020MS05063), and the Inner Mongolia Science and Technology Plan Project, China (No. 2020GG0230).

References

[1] LI Jia-yan, WANG Jin-man. Comprehensive utilization and environmental risks of coal gangue: A review [J]. Journal of Cleaner Production, 2019, 239: 117946−117963.

[2] XUE Jian-qiang, LIU Jian-xin, HUANG De-zhi, ZHOU Wei-jian, LIU Chun-ming, CAO Yu-sen, CAO Chuang-hua. Sources of rare earth elements REE+Y (REY) in Bayili Coal Mine from Wensu County of Xinjiang, China [J]. Transactions of Nonferrous Metals Society of China, 2021, 31: 3105−3115.

[3] ZHANG Rui, WU Kai, JIANG Zheng-wu, WANG Jian-yun. Bacterially induced $CaCO_3$ precipitation for the enhancement of quality of coal gangue [J]. Construction and Building Materials, 2022, 319: 126102−126111.

[4] SUN Ya-qiao, XIAO Kang, WANG Xiao-dong, LV Zi-hao, MAO Ming. Evaluating the distribution and potential ecological risks of heavy metal in coal gangue [J]. Environmental Science and Pollution Research International, 2021, 28: 18604−18615.

[5] ZHOU Chun-cai, LIU Gui-jian, WU Sheng-chun, LAM P K S. The environmental characteristics of usage of coal gangue in bricking-making: A case study at Huainan, China [J]. Chemosphere, 2014, 95: 274−280.

[6] LUO Li-qun, LI Ke-yao, FU Weng, LIU Cheng, YANG Si-yuan. Preparation, characteristics and mechanisms of the composite sintered bricks produced from shale, sewage sludge, coal gangue powder and iron ore tailings [J]. Construction and Building Materials, 2020, 232:

117250−117257.

[7] XIAO Jin, LI Fa-chuang, ZHONG Qi-fan, BAO Hong-guang, WANG Bing-jie, HUANG Jin-di, ZHANG Yan-bing. Separation of aluminum and silica from coal gangue by elevated temperature acid leaching for the preparation of alumina and SiC [J]. Hydrometallurgy, 2015, 155: 118−124.

[8] CHENG Wei, BIAN Zheng-fu, DONG Ji-hong, LEI Shao-gang. Soil properties in reclaimed farmland by filling subsidence basin due to underground coal mining with mineral wastes in China [J]. Transactions of Nonferrous Metals Society of China, 2014, 24: 2627−2635.

[9] GUAN Xiao, CHEN Ji-xi, ZHU Meng-yu, GAO Jie. Performance of microwave-activated coal gangue powder as auxiliary cementitious material [J]. Journal of Materials Research and Technology, 2021, 14: 2799−2811.

[10] WU Chang-liang, JIANG Wen, ZHANG Chao, LI Jing-wei, WU Shuang, WANG Xu-jiang, XU Yi-meng, WANG Wen-long, FENG Mei-jun. Preparation of solid-waste-based pervious concrete for pavement: A two-stage utilization approach of coal gangue [J]. Construction and Building Materials, 2022, 319: 125962−125975.

[11] CAO Peng-xu, LI Guang-hui, JIANG Hao, ZHANG Xin, LUO Jun, RAO Ming-jun, JIANG Tao. Extraction and value-added utilization of alumina from coal fly ash via one-step hydrothermal process followed by carbonation [J]. Journal of Cleaner Production, 2021, 323: 129174−129182.

[12] HAN Li-na, REN Wei-guo, WANG Bing, HE Xing-xing, MA Ling-jun, HUO Qi-huang, WANG Jian-cheng, BAO Wei-ren, CHANG Li-ping. Extraction of SiO_2 and Al_2O_3 from coal gangue activated by supercritical water [J]. Fuel, 2019, 253: 1184−1192.

[13] JIN Jian-ping, LIU Xiao, YUAN Shuai, GAO Peng, LI Yan-jun, ZHANG Hao, MENG Xiang-zhi. Innovative utilization of red mud through co-roasting with coal gangue for separation of iron and aluminum minerals [J]. Journal of Industrial and Engineering Chemistry, 2021, 98: 298−307.

[14] GUO Yan-xia, LV Hui-bin, YANG Xi, CHENG Fan-qin. $AlCl_3·6H_2O$ recovery from the acid leaching liquor of coal gangue by using concentrated hydrochloric inpouring [J]. Separation and Purification Technology, 2015, 151: 177−183.

[15] LUO Jun, LI Guang-hui, JIANG Tao, PENG Zhi-wei, RAO Ming-jun, ZHANG Yuan-bo. Conversion of coal gangue into alumina, tobermorite and TiO_2-rich material [J]. Journal of Central South University, 2016, 23: 1883−1889.

[16] YANG Quan-cheng, ZHANG Fan, DENG Xing-jian, GUO Hong-chen, ZHANG Chao, SHI Chang-sheng, ZENG Ming. Extraction of alumina from alumina rich coal gangue by a hydro-chemical process [J]. Royal Society Open Science, 2020, 7: 192132−192143.

[17] JIANG Zhou-qing, YANG Jing, MA Hong-wen, WANG Le, MA Xi. Reaction behaviour of Al_2O_3 and SiO_2 in high alumina coal fly ash during alkali hydrothermal process [J]. Transactions of Nonferrous Metals Society of China, 2015, 25: 2065−2072.

[18] GUO Yan-xia, YAN Ke-zhou, CUI Li, CHENG Fang-qin. Improved extraction of alumina from coal gangue by surface mechanically grinding modification [J]. Powder Technology, 2016, 302: 33−41.

[19] ZHAO Ji-hui, WANG Dong-min, LIAO Shu-cong. Effect of mechanical grinding on physical and chemical characteristics of circulating fluidized bed fly ash from coal gangue power plant [J]. Construction and Building Materials, 2015, 101: 851−860.

[20] LI Xiao-bin, WANG Hong-yang, ZHOU Qiu-sheng, QI Tian-gui, LIU Gui-hua, PENG Zhi-hong. Efficient separation of silica and alumina in simulated CFB slag by reduction roasting-alkaline leaching process [J]. Waste Management, 2019, 87: 798−804.

[21] SUN Xiao-xue, SUN Yu-zhu, YU Jiang-guo. Leaching of aluminum from coal spoil by mechanothermal activation [J]. Frontiers of Chemical Science and Engineering, 2015, 2: 216−223.

[22] CAO Zhao, CAO Yong-dan, DONG Hong-juan, ZHANG Jin-shan, SUN Chun-bao. Effect of calcination condition on the microstructure and pozzolanic activity of calcined coal gangue [J]. International Journal of Mineral Processing, 2016, 146: 23−28.

[23] ZHANG Ying-yi, XU Ling, SEETHARAMAN S, LIU Li-li, WANG Xi-dong, ZHANG Zuo-tai. Effects of chemistry and mineral on structural evolution and chemical reactivity of coal gangue during calcination: Towards efficient utilization [J]. Materials and Structures, 2015, 48: 2779−2793.

[24] LI Li-xin, ZHANG Yin-min, ZHANG Yong-feng, SUN Jun-min, HAO Zhi-fei. The thermal activation process of coal gangue selected from Zhungeer in China [J]. Journal of Thermal Analysis & Calorimetry, 2016, 126: 1559−1566.

[25] GUO Yan-xia, YAN Ke-zhou, CUI Li, CHENG Fang-qin, LOU H H. Effect of Na_2CO_3 additive on the activation of coal gangue for alumina extraction [J]. International Journal of Mineral Processing, 2014, 131: 51−57.

[26] DONG Ling, LIANG Xin-xing, SONG Qiang, GAO Ge-wu, SONG Li-hua, SHU Yuan-feng, SHU Xin-qian. Study on Al_2O_3 extraction from activated coal gangue under different calcination atmospheres [J]. Journal of Thermal Science, 2017, 26(6): 570−576.

[27] ZHENG Guang-ya, XIA Ju-pei, LIU Cheng-long, LI Wan-lin, YANG Jin, FAN Hui. Dissolution of aluminum and titanium during high-temperature acidification of coal gangues and relative kinetics [J]. Energy Sources, Part A: Recovery, Utilization, and Environmental Effects, 2019, 7: 1−14.

[28] LIN Min. LIU Yuan-yuan, LEI Shao-min, YE Zhao, PEI Zhen-yu, LI Bo. High-efficiency extraction of Al from coal-series kaolinite and its kinetics by calcination and pressure acid leaching [J]. Applied Clay Science, 2018, 161: 215−224.

[29] LI Bei, LIU Gang, GAO Wei, CONG Hai-yong, BI Ming-shu, MA Li, DENG Jun, SHU Chi-min. Study of combustion behaviour and kinetics modelling of Chinese Gongwusu coal gangue: Model-fitting and model-free approaches [J]. Fuel, 2020, 268: 117284−117295.

[30] VALEEV D, KUNILOVA I, SHOPPERT A, SALAZAR-CONCHA C, KONDRATIEV A. High-pressure HCl leaching of coal ash to extract Al into a chloride solution with further use as a coagulant for water treatment [J]. Journal of Cleaner Production, 2020, 276: 123206−123242.

[31] VALEEV D, MIKHAILOVA A, ATMADZHIDI A. Kinetics of iron extraction from coal fly ash by hydrochloric acid

leaching [J]. Metals, 2018, 8: 533−541.
[32] JOHNSTON C J, PEPPER R A, MARTENS W N, COUPERTHWAITE S. Improvement of aluminium extraction from low-grade kaolinite by iron oxide impurities: Role of clay chemistry and morphology [J]. Minerals Engineering, 2022, 176: 107346−107354.
[33] YANG Qun, LI Qi, ZHANG Guo-fan, SHI Qing, FENG Hai-gang. Investigation of leaching kinetics of aluminum extraction from secondary aluminum dross with use of hydrochloric acid [J]. Hydrometallurgy, 2019, 187: 158−167.
[34] RIVERA R M, XAKALASHE B, OUNOUGHENE G, BINNEMANS K, FRIEDRICH B, van GERVENA T. Selective rare earth element extraction using high-pressure acid leaching of slags arising from the smelting of bauxite residue [J]. Hydrometallurgy, 2019, 184: 162−174.
[35] VALEEV D, PANKRATOV D, SHOPPERT A, SOKOLOV A, KASIKOV A, MIKHAILOVA A, SALAZAR-CONCHA C, RODIONOV I. Mechanism and kinetics of iron extraction from high silica boehmite−kaolinite bauxite by hydrochloric acid leaching [J]. Transactions of Nonferrous Metals Society of China, 2021, 31: 3128−3149.
[36] VALEEV D V, LAINER Y A, MIKHAILOVA A B, DOROFIEVICH I V, ZHELEZNYI M V, GOL'DBERG M A, KUTSEV S V. Reaction of bauxite with hydrochloric acid under autoclave conditions [J]. Metallurgist, 2016, 60: 204−211.
[37] ZHANG Lei, WANG Hao, LI Yu. Research on the extract Al_2O_3 from coal gangue [J]. Advanced Materials Research, 2012, 524/525/526/527: 1947−1950.
[38] CHENG Fang-qin, CUI Li, MILLER J D, WANG X. Aluminum leaching from calcined coal waste using hydrochloric acid solution [J]. Mineral Processing and Extractive Metallurgy Review, 2012, 33: 391−403.
[39] XIE Ming-zhuang, LIU Feng-qin, ZHAO Hong-liang, KE Chao-yang, XU Zhi-qian. Mineral phase transformation in coal gangue by high temperature calcination and high-efficiency separation of alumina and silica minerals [J]. Journal of Materials Research and Technology, 2021, 14: 2281−2288.
[40] LI Xiao-bin, WANG Hong-yang, ZHOU Qiu-sheng, QI Tian-gui, LIU Gui-hua, PENG Zhi-hong, WAN Yi-lin. Reaction behavior of kaolinite with ferric oxide during reduction roasting [J]. Transactions of Nonferrous Metals Society of China, 2019, 29: 186−193.

煤矸石中氧化铝盐酸浸出动力学

张宇娟[1,2]，孙俊民[1,2]，吕国志[3]，张廷安[3]，公彦兵[1,2]

1. 内蒙古工业大学 化工学院，呼和浩特 010051；
2. 煤基固废高值化利用国家地方联合工程研究中心，呼和浩特 010051；
3. 东北大学 特殊冶金与过程工程研究所，多金属共生矿生态化冶金教育部重点实验室，沈阳 110819

摘　要：研究用盐酸从煤矸石中提取氧化铝的浸出动力学，并研究焙烧活化温度和浸出条件对氧化铝提取率的影响。实验结果表明，在最佳煅烧温度 700 ℃、浸出温度 150 ℃、反应 2 h、盐酸浓度 20%和液固比 3:1 的条件下，氧化铝提取率可达 91.56%，随着氧化铝的浸出，锂的协同浸出率可同时达到 80.00%。研究表明，氧化铝浸出过程符合收缩未反应核模型，且受化学反应控制，反应活化能为 45.64 kJ/mol。

关键词：煤矸石；酸浸；煅烧活化；浸出动力学；氧化铝

(Edited by Xiang-qun LI)